arXiv:0804.1664v1 [physics.atm-clus] 10 Apr 2008

Global Potential Energy Minima of $(H_2O)_n$ Clusters on Graphite: A Comparative Study of the TIPNP ($N = 3,\ 4,\ 5$) Family

B. S. González, J. Hernández-Rojas, J. Bretón, and J. M. Gomez Llorente*
Departamento de Física Fundamental II
Universidad de La Laguna, 38205 Tenerife, Spain

April 10, 2008

Abstract

The water-graphite interaction potential proposed recently (González et al. *J. Phys. Chem. C* **2007**, *111*, 14862), the three TIPNP ($N = 3$, 4, 5) water-water interaction models, and basin-hopping global optimization are used to find the likely candidates for the global potential energy minima of $(H_2O)_n$ clusters with $n \leq 21$ on the (0001)-surface of graphite and to perform a comparative study of these minima. We show that, except for the smaller clusters ($n < 6$), for which ab-initio results are available, the three water-water potential models provide mostly inequivalent conformations. While TIP3P seems to favor monolayer water structures for $n < 18$, TIP4P and TIP5P favor bilayer or volume structures for $n > 6$. These n values determine the threshold of dominance of the hydrophobic nature of the water-graphite interaction at the nanoscopic scale for these potential models.

1 Introduction

The interaction between water and graphite has been the concern of theoretical and experimental studies. A deep understanding of the features and properties of this interaction is of great interest in technological applications [1, 2, 3], environmental sciences [4], and

---

*Corresponding author. *E-mail address*: jmgomez@ull.es astrophysics [5], among other fields. The establishment of either the hydrophilic or hydrophobic nature of graphite at nanoscopic scales, which is of particular relevance in those applications, must be based on the knowledge of this interaction.

In a previous publication [6] (hereafter referred to as I), we have developed a model for the water-graphite interaction and found the likely candidates for the global potential energy minima of $(H_2O)_n$ clusters with $n \leq 21$ on the (0001)-surface of graphite. Out of this model, we have obtained a rather hydrophobic water-graphite interaction at the nanoscopic scale. As a consequence of this property, the water component of the lowest graphite-$(H_2O)_n$ minima is quite closely related to low-lying minima of the corresponding $(H_2O)_n$ clusters. In about half of the cases the geometrical substructure of the water molecules in the graphite-$(H_2O)_n$ global minimum coincides with that of the corresponding free water cluster. Exceptions occur when the interaction with graphite induces a change in the geometry of the water moiety. Our general conclusions were in agreement with the sparse experimental [7, 8] and theoretical data [3, 9, 10, 11, 12]. Besides, the structures of these minima for $1 < n \leq 6$ coincided with those provided by empirical [10] and ab initio calculations [3, 11].

In our study, the water-water interaction was described by the TIP4P intermolecular potential model [13]. The related TIP3P potential [13] was also used to model this interaction for $n \leq 6$. The global minimum structures found for these clusters coincided with those of the TIP4P model. However, the observed dependence of the structure of the water-graphite global minima on the structure of the corresponding free water clusters and the known dependence of the latter on the water-water interaction model for $n > 6$ anticipated a dependence of the structure of these larger water-graphite clusters on the form chosen to model the water-water interaction. In I, preliminary results with the TIP3P model confirmed this prediction. In this article, we will present the concluding results from our analysis of this dependence by considering also the TIP5P model [14]. As in I, we will make use of the water-graphite interaction model developed there and the basin-hopping method to find the likely candidates for the global potential energy minima of graphite-$(H_2O)_n$ clusters with $n \leq 21$ and the TIP3P and TIP5P water-water interaction models, and perform a systematic comparison of the cluster structures found with these and the TIP4P model.

This paper is organized as follows. In Section 2 we summarize the relevant details of the model developed in I for the water-graphite interaction. In Section 3 we present likely candidates for the cluster global potential energy minima together with their association and binding energies for both the TIP3P and TIP5P water-water interaction models. We shall also compare these global minimum structures with those found in I for the TIP4P model. Finally, Section 4 summarizes our conclusions.

2 Summary of the Potential Energy Function

The closed-shell electronic structure of both graphite and water makes an empirical approach to the potential energy surface (PES) for the water-graphite and water-water interactions particularly attractive. In I, we wrote the potential energy of a graphite-$(H_2O)_n$ cluster as a sum of two contributions

$$V = V_{\mathrm{ww}} + V_{\mathrm{wg}}, \tag{1}$$

where V_{ww} is the sum of pairwise water-water interactions, and V_{wg} is the water-graphite term. For the water-water interaction, the TIP4P model was the primary choice in I; here we will study the performance of the TIP3P and TIP5P potentials. All these models describe each water molecule as the same rigid body with two positive charges on the hydrogen atoms and either a balancing negative charge at the oxygen atom (TIP3P) or close to the oxygen atom (TIP4P), or two balancing negative charges close to the oxygen atom and out of the molecular plane (TIP5P), together with a dispersion-repulsion center on the oxygen atom. Hence, $V_{\rm ww}$ is a sum of pairwise additive Coulomb and Lennard-Jones terms. We should remind here that the TIPNP are a family of empirical water-water potentials whose parameters have been appropriately set so as to reproduce some properties of the liquid water phase at room temperature. Potentials from these family have been used in the study of homogeneous water clusters [15, 16, 17, 18], water clusters containing metallic cations [19, 20], and water-C_{60} clusters [21].

The water-graphite interaction is written as

$$V_{\rm wg} = V_{\rm dr} + V_{\rm pol}, \tag{2}$$

where $V_{\rm dr}$ is a sum of pairwise dispersion-repulsion terms between the oxygen and the carbon atoms. Each of these terms is expressed as a Lennard-Jones potential, whose parameters were obtained using the standard Lorentz-Berthelot combination rules from the corresponding parameters for the oxygen-oxygen and carbon-carbon interactions in TIPNP water and Steele [22] graphene-graphene potentials, respectively. Specifically, we used the values $\varepsilon_{\rm CO} = 0.385$ kJ/mol and $\sigma_{\rm CO} = 3.28\,\text{Å}$ for the TIP3P, and $\varepsilon_{\rm CO} = 0.395$ kJ/mol and $\sigma_{\rm CO} = 3.26\,\text{Å}$ for the TIP5P (see [6] for TIP4P parameters), which are similar to those derived by Werder *et al.* [9] to fit the contact angle for a water droplet on a graphene surface. A simple analytic form for $V_{\rm dr}$ can be obtained using Steele summation method [22, 23] over the graphite periodic structure by writing the interaction of a dispersion center with a graphite layer as a Fourier series. The total repulsion-dispersion interaction is obtained as a sum of such terms over each graphite layer. We have obtained well converged values by including the continuum contribution from the two upper layers and the first corrugation from the first layer.

In Eq. (2), V_{pol} includes the energy associated with the polarization of graphite due to the electric field of all the water point charges. This many-body interaction, which turns out to be smaller than V_{dr}, was evaluated using a continuous representation of graphite in terms of two contributions,

$$V_{\mathrm{pol}} = V_{\|} + V_{\perp}, \tag{3}$$

each one associated, respectively, with the response of graphite to the electric field component parallel and perpendicular to the graphite surface. For the first one, $V_{\|}$, we assumed that graphite behaves as a classical conductor, which allowed us to make use of the image charge method to obtain its analytical form. In order to evaluate $V_{\perp}$, we associated to the graphite surface a constant surface polarizability density $\alpha_{\perp}$ such that when an electric field depending on the surface point and perpendicular to the layer, $E_{\perp}(x, y)$, is applied, an electric dipole density, $I(x, y)$, is induced on that layer, with $I(x, y) = \alpha_{\perp} E_{\perp}(x, y)$. Using image charge methods one readily shows that if the graphite surface coincides with the plane $z = 0$, the induced image of an electric charge q_i at the point (x_i, y_i, z_i) is an electric dipole $p_i = -2\pi\alpha_{\perp} q_i$ at the point $(x_i, y_i, -z_i)$ and direction parallel to the z axis. This result can be generalized additively to the case of several electric point charges to obtain an analytical form for $V_{\perp}$. The value of the polarizability density $\alpha_{\perp}$ was estimated from $\varepsilon_{\perp}$, the relative electric permittivity of graphite for applied electric fields perpendicular to the (0001) surface, whose value is $\varepsilon_{\perp} = 5.75$; namely,

$$\alpha_{\perp} = \frac{d(\varepsilon_{\perp} - 1)}{4\pi\varepsilon_{\perp}}, \tag{4}$$

where $d = 3.35$ Å is the graphite interlayer distance. We obtained by this procedure $\alpha_{\perp} = 0.220$ Å.

All other electrostatic contributions to the water-graphite interaction energy having vanishing continuous terms (as the water-charge carbon-quadrupole interaction) have been neglected, as well as the McLachlan substrate mediated water-water interaction [25]. This potential energy surface was argued to be superior to previous empirical models [10].

3 Global Potential Energy Minima

Likely candidates for the global potential energy minima of graphite-$(H_2O)_n$ clusters with $n \leq 21$ were located using the basin-hopping scheme [26], which corresponds to the 'Monte Carlo plus energy minimization approach of Li and Scheraga [27]. This method has been used successfully for both neutral [26] and charged atomic and molecular clusters [21, 28, 29, 30, 31], along with many other applications [32]; of course, this was the method used in I. In the size range considered here the global optimization problem is relatively straightforward. The global minimum is generally found in fewer than 7×10^4 basin-hopping steps, independently of the random starting geometry. In some cases, starting out from the $(H_2O)_n$ global potential minimum, the corresponding global minimum for graphite-$(H_2O)_n$ is found even faster. However, the success hit rate of the optimization method decreases significantly and the likelihood of our candidates decreases. As a matter of fact, we have been able to find for $n = 19$ and $n = 21$, in each case, a TIP4P global minimum candidate with energy lower than the one found in I; although these new candidates present structures very similar to the previously reported ones.

For graphite-$(H_2O)_n$ clusters, association energies, ΔE_a, are defined for the process

$$\text{graphite} + n\mathrm{H_2O} = \text{graphite-}(\mathrm{H_2O})_n; \qquad -\Delta E_\mathrm{a}. \tag{5}$$

We also define the water binding energy, ΔE_b, as the difference between the association energies of graphite-$(H_2O)_n$ and $(H_2O)_n$; that is,

$$\text{graphite} + (\mathrm{H_2O})_n = \text{graphite-}(\mathrm{H_2O})_n; \qquad -\Delta E_\mathrm{b}. \tag{6}$$

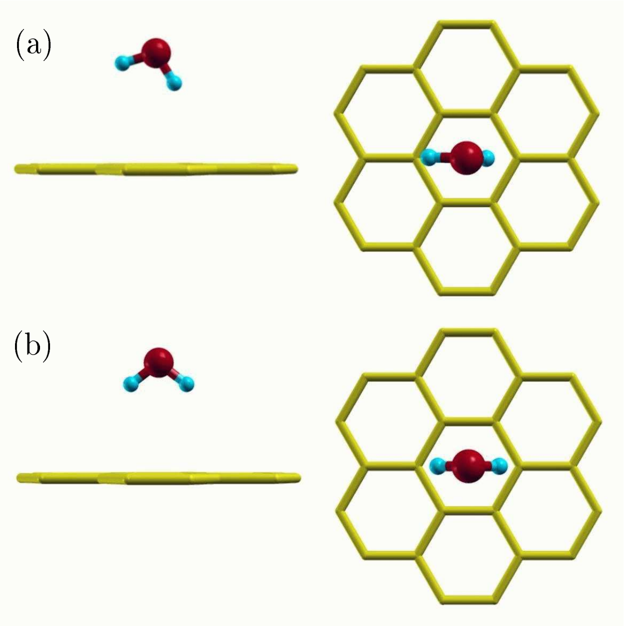

Figure 1: Two views of the global minimum obtained for graphite-(H_2O). Water-water potential models: TIP3P (a); TIP5P (b). This figure, as well as figures 4 and 5, was prepared using the program XCrysDen [36].

The clusters in these expressions are assumed to be in their global minimum. The structures and association energies employed here for the global minima of $(H_2O)_n$ coincide precisely with those obtained by Wales and Hodges [15], Kabrede and Hentschke [16], and James et al. [18].

In the water monomer case, the structures found for the water-graphite system with the TIP3P and TIP5P potentials are given in Fig. 1 (those for TIP4P were presented in I). While TIP3P, as well as TIP4P [6], favors a one-legged structure, the TIP5P model produces a two-legged global minimum. The equilibrium distance in the global minimum between the oxygen and the graphite surface is 3.13 Å for the TIP3P potential and 3.12 Å for the other two models; these distances are very close to the *ab initio* value (3.04 Å) [11] and the corresponding values in water-C_{60} (3.19 Å) [21] and water-benzene (experimental, 3.33 Å) [33]. As happens with the TIP4P model, one-legged and two-legged stable structures exist very close in energy for each of the TIPNP models. Therefore, as we

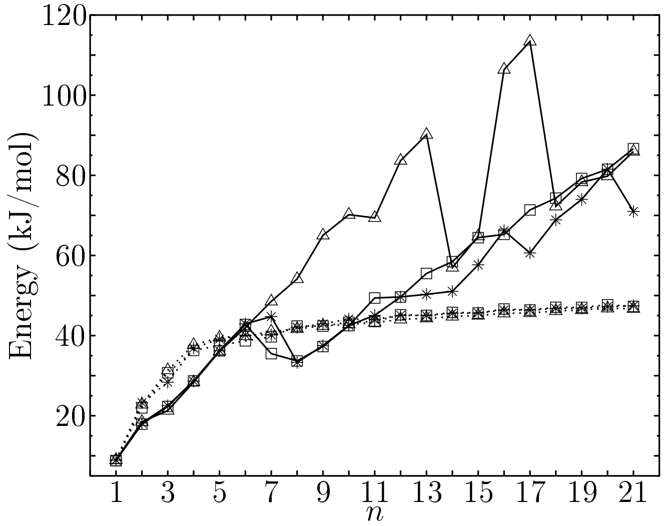

Figure 2: Binding, ΔE_{b} (full lines), and association, $\Delta E_{\mathrm{a}}/n$ (dotted lines), energies in kJ/mol for the global minima of water-graphene clusters: TIP3P (triangles), TIP4P (squares), TIP5P (stars).

have discussed in I, the structures found here for the water monomer might change by the inclusion in our potential energy surface of the corrugation terms associated with the electrostatic interactions, which have been neglected in our PES. For instance, the carbon-quadrupole contribution may favor a two-legged structure [34]. However, these effects will tend to average out in the adsorption of water clusters.

The three model potentials provide very similar monomer binding energies, namely $\Delta E_{\mathrm{b}} = 8.81\,\mathrm{kJ/mol}$ for the TIP4P and $\Delta E_{\mathrm{b}} = 8.94\,\mathrm{kJ/mol}$ for the other two models, in good agreement with the ab-initio data. The contribution of the polarization energy to these binding energies ($\sim 25\%$) follows the same trend as the magnitude of the water dipole moment for each model and it is responsible for the orientation of the H_2O molecule on the graphite surface.

The association ($\Delta E_{\mathrm{a}}/n$) and binding energies (ΔE_{b}) for the full graphite-$(H_2O)_n$ clusters obtained for the three TIPNP water-water interactions are given in Table 1 and plotted in Fig. 2. We also show in Fig. 3 the values of the polarization energy V_{pol} and water-graphite dispersion-repulsion energy V_{dr}, as defined in Section 2, for the cluster global

Table 1: Global minimum association and binding energies in kJ/mol.

n	TIP3P		TIP4P		TIP5P		Equivalences
	ΔE_{a}	ΔE_{b}	ΔE_{a}	ΔE_{b}	ΔE_{a}	ΔE_{b}	
2	-45.641	-18.495	-43.921	-17.909	-46.557	-18.173	3P, 4P, 5P
3	-94.128	-21.292	-92.182	-22.317	-85.108	-22.521	3P, 4P, 5P
4	-150.719	-28.388	-145.199	-28.708	-147.586	-28.650	3P, 4P, 5P
5	-197.572	-36.069	-187.683	-36.220	-195.660	-36.262	3P, 4P, 5P
6	-239.280	-42.001	-232.207	-42.773	-240.824	-42.918	3P, 4P
7	-287.249	-48.535	-277.938	-35.512	-281.399	-44.749	3P, 5P
8	-333.402	-54.132	-339.035	-33.686	-336.466	-33.311	4P, 5P
9	-382.078	-65.013	-381.527	-37.277	-386.252	-37.510	4P, 5P
10	-428.329	-70.183	-433.315	-42.486	-441.510	-42.560	4P, 5P
11	-475.783	-69.380	-478.621	-49.388	-483.825	-45.044	
12	-528.547	-83.655	-542.278	-49.645	-540.978	-49.660	
13	-576.331	-90.123	-585.446	-55.506	-584.911	-50.291	
14	-626.761	-56.986	-641.126	-58.448	-638.105	-51.048	3P, 4P
15	-675.072	-64.806	-684.664	-64.439	-684.710	-57.668	4P, 5P
16	-728.942	-106.378	-746.178	-65.272	-742.269	-66.191	
17	-776.162	-113.412	-788.699	-71.355	-788.253	-60.630	
18	-830.627	-72.256	-847.050	-74.300	-841.842	-68.892	
19	-881.578	-78.300	-894.134	-79.740	-890.437	-73.994	3P, 4P
20	-935.993	-79.786	-953.950	-81.513	-944.519	-81.551	4P, 5P
21	-980.995	-85.926	-993.960	-87.051	-996.230	-70.984	3P, 4P

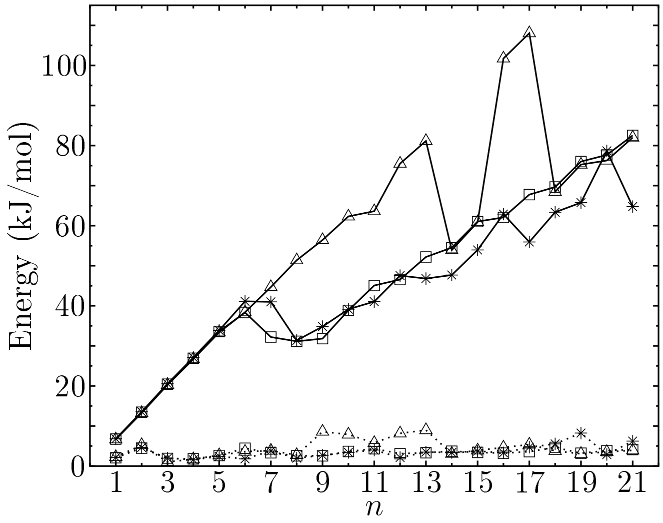

Figure 3: Dispersion-repulsion, V_{dr} (full line), and Polarization, V_{pol} (dotted line), contributions to the binding energies in kJ/mol: TIP3P (triangles), TIP4P (squares), TIP5P (stars).

minima. The three water-water potential models provide very similar values for the association energies. However, the binding energies for TIP4P and TIP5P models differ significantly from those obtained with the TIP3P for $n > 6$. The origin of this difference is, as can be seen in Fig. 3, in the V_{dr} term, which is the dominant contribution for $n > 2$. The term V_{pol} oscillates with n around an average value of $\overline{V}_{\mathrm{pol}} = 3.5\,\mathrm{kJ/mol}$; the two contributions to V_{pol}, $V_{\parallel}$ and $V_{\perp}$, are similar in magnitude with $V_{\parallel}$ somewhat larger than $V_{\perp}$. The term V_{dr} fluctuates also around a slowly growing average as the number of water molecules close to the graphite surface increases. On average, each of these water molecules contributes about 7.3 kJ/mol to V_{dr}. The water-graphite binding energies correspond quite closely to the sum of V_{pol} and V_{dr}, while the association energies are dominated by the water-water interaction. The average value of the association energy per molecule in homogeneous TIPNP $(H_2O)_n$ clusters with $6 \leq n \leq 21$ is $\sim 42\,\mathrm{kJ/mol}$ [15, 16]. For water cluster on graphite the corresponding value turns out to be 44.6 kJ/mol, which is comparable with the experimental value of $43.4 \pm 2.9\,\mathrm{kJ/mol}$ [7]. Any of these values corresponds to the binding energy of a water molecule in a water cluster, and it is much larger than the energy for binding a water molecule onto the graphite surface. This energy balance would support an hydrophobic nature of the water-graphite interaction at large scale, as we have already discussed in I.

The structures of the TIP3P lowest minima obtained for graphite-$(H_2O)_n$ are presented in Fig. 4, and those of the TIP5P in Fig. 5 (The corresponding TIP4P global minima were presented in I). The three water-water model potentials provide practically identical structures for $2 \leq n \leq 5$. The water substructures in these compounds are actually equivalent (see below) to those in the corresponding free global minimum of TIPNP $(H_2O)_n$ [15, 16, 18], and are in agreement with the ab-initio results. For $n = 6$, TIP3P and TIP4P model have a "book" global minimum, as the one predicted by ab-initio calculations [3, 11], while the TIP5P leads to an hexagonal ring. This result would favor the first two models over the last one. Only the water substructure in the TIP4P differs from that of the corresponding free water cluster global minimum ("cage" conformation).

Here, we will consider two global minima equivalent if their water moieties share the same geometrical structure (aside from minor differences in angles and distances) and orientation with respect to the graphite surface plane With this convention the equivalences found in the global minima of graphite-$(H_2O)_n$ compounds among the three PES have been included in the last column of Table 1. The number of these equivalences is similar to the number of equivalences between the three model potentials in the corresponding free water clusters, although these equivalences involve different clusters and potentials. For instance, TIP3P and TIP5P provide equivalent free water global minima for $n = 8$; both models present the D_{2d} "cube" conformation, while TIP4P global minimum has an S_4 "cube" conformation. On the other hand, the corresponding water clusters on graphite keep the free structure for TIP4P and TIP5P, while TIP3P provides a monolayer water conformation; therefore no equivalent structures appear in this case.

For graphite-water clusters with $6 < n \leq 17$, the TIP3P model seems to favor monolayer

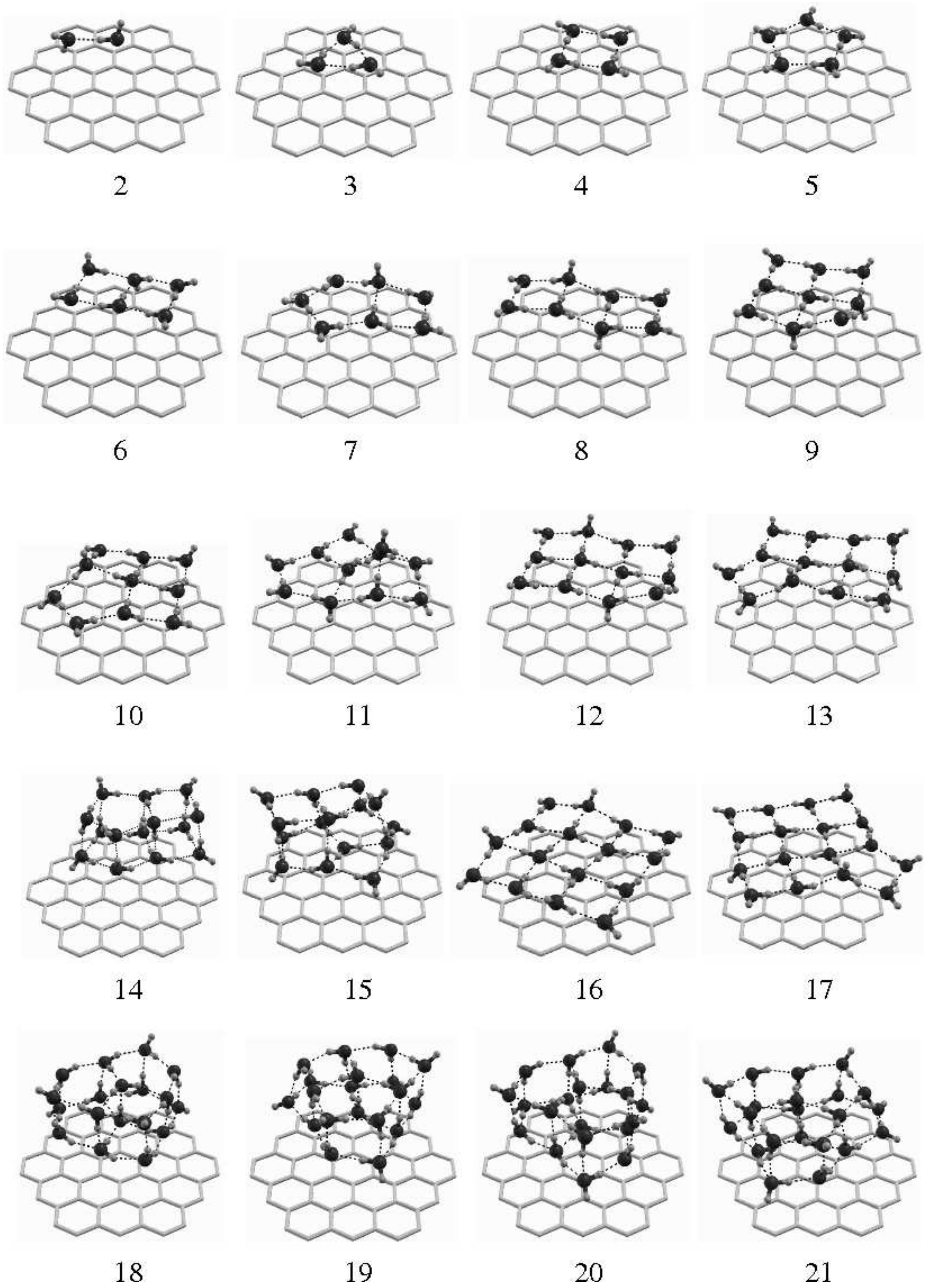

2 3 4 5

6 7 8 9

10 11 12 13

14 15 16 17

18 19 20 21

Figure 4: Likely global minima obtained for graphite-$(H_2O)_n$ clusters with the TIP3P water-water potential model.

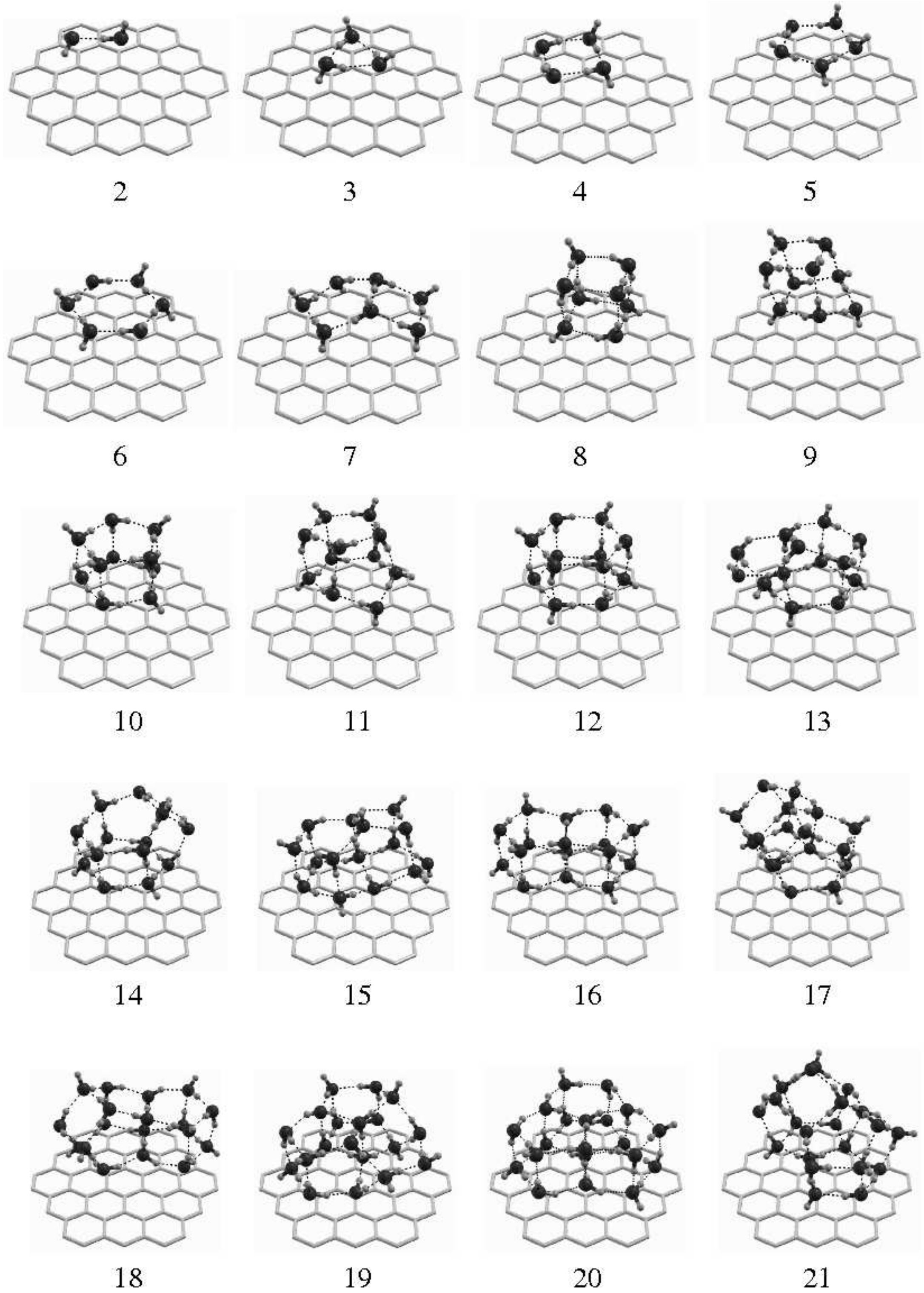

Figure 5: Likely global minima obtained for graphite-$(H_2O)_n$ clusters with the TIP5P water-water potential model.

water structures (with exceptions for $n = 14$ and 15), while the other two models favor either bilayer (TIP4P and TIP5P) or volume (only TIP5P) structures. The exceptions to the monolayer pattern for $n = 14, 15$ in TIP3P, may be explained by the relative higher stability (deduced from second energy differences) of the corresponding free water clusters respect to that of their neighbors $n = 13, 16$. For $17 < n \leq 21$, either volume or bilayer conformations are found for the three model potentials.

When we compare the conformation of the water substructure on the graphite surface with that of the corresponding free water cluster, we find also a markedly different behavior for the TIP3P model. With the exception of the first six clusters and the case $n = 14$, those two conformations are inequivalent. In other word, the water-graphite interaction is able to strongly modify the structure of the free water clusters. This together with the monolayer conformation of the adsorbed water clusters would point out to a hydrophilic water-graphite interaction for this potential model. However this behavior seem to be due to finite size effects since we have not found monolayer global minimum structures for $n > 17$, neither local minima monolayer conformations that are close in energy to the global minima. For $n > 6$ in TIP4P and $n > 7$ in TIP5P, we do not find either such monolayer structures for these two potential models. Thus the hydrophobic nature of the water-graphite interaction appears earlier in these models. Furthermore, in some cases for the two latter models, the conformation of the water substructure on graphite and that of the corresponding free water cluster are equivalent. The exceptions are $n =$ 6, 7, 11, 15, 17, 19, 21 for TIP4P and $n =$ 7, $n \geq 13$ for TIP5P. In these cases, the water substructure is equivalent to a low-lying local minimum of the corresponding TIPNP $(H_2O)_n$ cluster, rather than to the global minimum. The energy penalty for this choice is mainly compensated by a more favorable dispersion-repulsion contribution to the interaction energy with graphite, which arises from a larger water-graphite contact area. In the structures for the three model potentials one finds square and pentagonal water rings; on the other hand, hexagonal rings are less common but they appear more often in TIP5P (n = 11, 12, 14, 15, 19) than in TIP3P and TIP4P (just for $n = 21$).

For TIP4P, the complete two-layer water structures for even n are precisely the structures of the global TIP4P free water clusters. Therefore, these structures interact with graphite in an optimal way and they keep their structure in the corresponding water-graphite clusters. On the other hand, for odd n, the free water global minima do not show optimal surfaces for its interaction with graphite, thus explaining why these clusters change their structure to minimize that interaction energy. The chosen new structures are sensibly determined by those of either the $n - 1$ or $n + 1$ clusters. The TIP5P (and also TIP3P) potential model do not produce this alternating behavior in the structure of the free water global minima and, therefore, we find a different behavior in the water-graphite global minima for $n \geq 8$.

Second energy differences account for the relative cluster stability; their values for association and binding energies, per water molecule, are plotted in Fig. 6. TIP4P and TIP5P, show practically the same behavior in the whole n range. The $n = 4$ cluster is particularly stable in all cases. For $n > 10$, we observe that the three model potentials present an oscillation of period $\Delta n = 2$, namely, clusters with even n are more stable than their odd n neighbors. This is an interesting feature because it does not occur so neatly for the free water clusters, and it is not obviously related, except in the TIP4P case [6], with the cluster structures. Second differences for the binding energies do not show common patterns for the three potential models because these provide very different global minima structures respect to the water-graphite interaction.

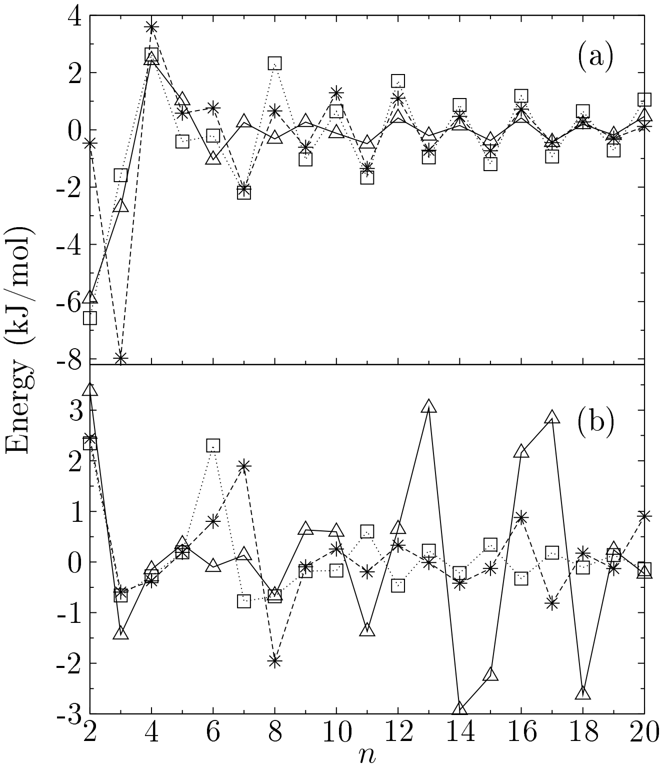

Figure 6: Second energy differences per water molecule (in kJ/mol) for the association energies (a) and binding energies (b) of water-graphite clusters. Water-water potential models: TIP3P (triangles, full line), TIP4P (squares, dotted line), TIP5P (stars, dashed line)

4 Conclusions

Using basin-hopping global optimization and a potential energy surface built up from three different water-water interaction models (TIP3P, TIP4P and TIP5P) we have characterized the geometrical structures and energetics of the likely candidates for the global potential energy minima of graphite-$(H_2O)_n$ clusters up to $n = 21$. The structures of these minima for $1 < n \leq 5$ coincide for the three potential models with those provided by other available calculations. The global minimum for the compound with $n = 6$ agrees with the ab-initio structure for TIP3P and TIP4P, but not for TIP5P. For $n > 6$, no ab-initio data are available and, except for the equivalences presented in Table I, the three model potentials provide different global minimum structures, as occurs for the free water clusters. For $n > 2$, association energies are dominated by the water-water interaction while the main contribution to the binding energies comes from the dispersion energy; furthermore the polarization term V_{pol} can be safely neglected for the larger clusters ($n > 3$); this justifies the use of water-graphite potentials that include only dispersion-repulsion terms [9]. For small n, the water grows on the graphite surface forming a monolayer. However, as n increases the hydrophobic nature of the water-graphite interaction dominates and breaks this tendency. The threshold for this transition is at $n = 7$ for TIP4P and TIP5P and $n = 18$ (with the exceptions $n = 14$, 15) for TIP3P. Therefore this latter potential seem to favor planar conformations up to larger n.

The hydrophobic character of the water-graphite interaction at the nanoscopic level makes in some cases the water substructure in the lowest energy clusters to be equivalent to a low-lying minimum of the appropriate $(H_2O)_n$ free cluster. In many cases the structure is simply a slightly relaxed version of the global minimum for $(H_2O)_n$, and therefore equivalent to it. For TIP3P this occurs only for the first six n values and for $n = 14$. TIP5P shows equivalences for the same first six n values and for $n = 8$, 9, 10, 11, 12. TIP4P shows the larger number of equivalences for $n \leq 5$ and $n = 8, 9, 10, 12, 13, 14, 16, 18, 20$.

The lowest energy structures obtained in the present work will be made available for download from the Cambridge Cluster Database [35].

Acknowledgments

This work was supported by ‘Ministerio de Educación y Ciencia (Spain)’ and ‘FEDER fund (EU)’ under contract No. FIS2005-02886. One of us (BSG) also aknowledges ‘Ministerio de Educación y Ciencia (Spain)’ for an FPU fellowship .

References

[1] Lancaster, J. K.; *Tribology Int.* **1990**, *23*, 371.

[2] Zaidi, H.; Paulmier D.; Lapage, J.; *Appl. Surf. Sci.* **1990**, *44*, 221.

[3] Xu, S.; Irle, S.; Musaev, A. G.; Lin, M. C. *J. Phys. Chem. A* **2005**, *109*, 9563.

[4] Popovicheva, O. P.; Persiantseva, N. M.; Trukhin M. E.; Rulev, G. B.; Shonija, N. K.; Buriko, I. I.; Starik, A. M.; Demirdjian, B.; Ferry, D.; Suzane, J. *Phys. Chem. Chem. Phys.* **2000**, *2*, 4421.

[5] Draine, B. T. *Annu. Rev. Astron. Astrophys.* **2003**, *41*, 241.

[6] González, B.S.; Hernández-Rojas, J.; Bretón, J; Gomez Llorente, J.M. *J. Phys. Chem. C* **2007**, *111*, 14862.

[7] Chakarov, D.; Österlund, L.; Kasemo, B. *Vacuum* **1995**, *46*, 1109. *Langmuir* **1995**, *11*, 1201.

[8] Avgul, N. N.; Kieslev, A. V. *Chemistry and Physics of Carbon*; Walker, P. L. Ed.; Dekker: New York, 1970, Vol. 6.

[9] Werder, T.; Walther, J. H.; Jaffe, R. L.; Halicioglu, T.; Koumoutsakos, P. *J. Phys. Chem. B* **2003**, *107*, 1345.

[10] Karapetian, K.; Jordan, K. D. *Water in Confined Environements*; Devling, J. P.; Buch, V., Eds.; Springer: New York, 2003; p. 139.

[11] Lin, C. S.; Zhang, R. Q.; Lee, S. T.; Elstner, M.; Frauenheim, Th.; Wan, L. J. *J. Phys. Chem. B* **2005**, *109*, 14183.

[12] Sudiarta, I. W.; Geldart, D. J. W. *J. Phys. Chem. A* **2006**, *110*, 10501.

[13] Jorgensen, W. L. *J. Chem. Phys.* **1982**, *77*, 4156.

[14] Mahoney, M.W.; Jorgensen, W.L. *J. Chem. Phys.* **2000**, *112*, 8910.

[15] Wales, D. J.; Hodges, M. P. *Chem. Phys. Lett.* **1998**, *286*, 65.

[16] Kabrede, H.; Hentschke, R. *J. Phys. Chem. B* **2003**, *107*, 3914.

[17] Hartke, B. *Z. Phys. Chem. B* **2000**, *214*, 1251.

[18] James, T.; Wales, D.J.; Hernández-Rojas, J. *Chem. Phys. Lett.* **2005**, *415*, 302.

[19] González, B. S.; Hernández-Rojas, J.; Wales, D. J. *Chem. Phys. Lett.* **2005**, *412*, 23.

[20] Schulz, F.; Hartke, B. *Chem. Phys. Chem.* **2002**, *3*, 98.

[21] Hernández-Rojas, J.; Bretón, J.; Gomez Llorente, J. M.; Wales, D. J. *J. Phys. Chem. B* **2006**, *110*, 13357.

[22] Steele, W. A. *The Interaction of Gases with Solid Surfaces*; Pergamon Press: Oxford, U.K., 1974.

[23] Ocasio, M.; López, G. E. *J. Chem. Phys.* **2000**, *112*, 3339.

[24] Hannay, J. H. *Eur. J. Phy.* **1983**, *4*, 141.

[25] Bruch, L. W.; Cole, M. W.; Zaremba, E. *Physical Adsorption: Forces and Phenomena*; Clarendon Press: Oxford, U.K., 1997.

[26] Wales, D. J.; Doye, J. P. K. *J. Phys. Chem. A* **1997**, *101*, 5111.

[27] Li, Z. Q.; Scheraga, H. A. *Proc. Natl. Acad. Sci. U.S.A.* **1987**, *84*, 6611.

[28] Doye, J. P. K.; Wales, D. J. *Phys. Rev. B* **1999**, *59*, 2292.

[29] Hernández-Rojas, J.; Wales, D. J. *J. Chem. Phys.* **2003**, *119*, 7800.

[30] Hernández-Rojas, J.; Bretón, J.; Gomez Llorente, J. M.; Wales, D. J. *J. Chem. Phys.* **2004**, *121*, 12315.

[31] Hernández-Rojas, J.; Bretón, J.; Gomez Llorente, J. M.; Wales, D. J. *Chem. Phys. Lett.* **2005**, *410*, 404.

[32] Wales, D. J. *Energy Landscapes*; Cambridge University Press: Cambridge, U.K., 2003.

[33] Gutowsky, H.S.; Emilsson, T.; Arunan, E. *J. Chem. Phys.* **1993**, *94*, 4883.

[34] Vernov, A.; Steele, W. A. *Langmuir* **1992**, *8*, 155.

[35] Wales, D. J.; Doye, J. P. K.; Dullweber, A.; Hodges, M. P.; Naumkin, F. Y.; Calvo, F.; Hernández-Rojas, J.; Middleton, T. F. The Cambridge Cluster Database, http://www-wales.ch.cam.ac.uk/CCD.html.

[36] Kokalj, A. *J. Mol. Graph. Model.* **1999**, *17*, 176.